EXPERIMENTAL AND NUMERICAL EVALUATION OF FORMING AND FRACTURE BEHAVIOUR OF HIGH STRENGTH STEEL

C. Nikhare[1], P. V. Marcondes[2], M. Weiss[1]* and P. D. Hodgson[1]

[1]*School of Engineering and Technology, Faculty of Science and Technology, Deakin University, Waurn Ponds 3217, Australia*
[2]*Universidade Federal do Paraná, DEMEC, Av. Cel. Francisco H. dos Santos, 210 CEP 81531-990, Curitiba, Paraná - Brazil*
*Corresponding author: matthias.weiss@deakin.edu.au

Abstract: Car manufacturers are under pressure to reduce vehicle mass while maintaining comfort and passenger safety for current and future vehicles. To meet this demand the steel industry has developed Advanced High Strength Steels (AHSS) that promise higher strength and improved formability compared to conventional steel grades. Even though significant research has already been performed to evaluate the material properties and forming behaviour of most AHSS types, only a limited literature is available on their necking and fracture behaviour and the effect on formability. This paper examines and compares the thinning, necking and fracture behaviour of two AHSS and one conventional steel type, namely TRIP, DP and HSLA. Uniaxial, plane and biaxial strain conditions are investigated by tensile, cup drawing and stretch forming tests and by using numerical methods. The test results indicate that significant differences exist in necking and fracture behaviour between all three steel types.

Keywords: AHSS modelling; fracture behaviour, thinning

Introduction

Environmental concerns are growing and encouraging automotive manufacturers to reduce the weight of future vehicles to achieve higher fuel economy and lower CO_2 gas emission. In addition, regulations to protect passengers in accidents are tightening. Advanced High Strength Steels (AHSS) are effective in thickness reduction of automotive parts without compromising the strength and crash performance and are therefore a promising solution if weight reduction in combination with increased safety is required [1].

ULSAB (Ultra Light Steel Auto Body) [2] has defined steels with an ultimate tensile strength greater than 700MPa as AHSS. They are generally multiphase steels that contain martensite, bainite and/or retained austenite in quantities sufficient to produce unique mechanical properties. AHSS generally exhibit an excellent combination of high strength and high formability resulting primarily from their high strain hardening capabilities [3-7]. However the material behaviour of AHSS is still not fully understood, and in sheet metal forming AHSS can show high and unpredictable springback as well as unpredictable and sudden failure, which is limiting their usage in some applications [8, 9].

In stamping of mild and conventional high strength steel, the typical failure mode is localized necking, resulting splitting. This type of failure can be related to critical levels of strain in a part [10]. Previous studies performed on Dual Phase (DP) steels have shown that the failure behaviour can be accurately described using FLD curves in cases where localised necking occurs [11-13]. However, in commercial stamping operations involving pronounced bending deformation, fractures have been observed that do not resemble localized necking. In these cases it was not possible to estimate the initiation of fracture using FLD curves [9, 14]. To be able to estimate the initiation of fracture for multiphase steels the necking and fracture behaviour of AHSS for different deformation modes needs to be studied.

Previous work has shown that the necking and fracture of steel is significantly influenced by the microstructure. While for conventional steel the necking and fracture properties are generally accurately represented by the mechanical properties obtained from the tensile test, for AHSS divergences have been observed between the forming behaviour indicated by the tensile test and

the actual material behaviour in sheet metal forming. It was further found that the effect of microstructure on the forming behaviour of AHSS depends on the forming path [15, 16]. This finding is especially important in finite element modelling since it suggests that the material behaviour of AHSS can be sufficiently represented by a simple material model based on tensile data for some forming applications while, depending on the forming path, for other forming applications more sophisticated material models based on the microstructure are required.

In this study the thinning, necking and fracture behaviour of two AHSS and one conventional steel type was studied. All steels showed similar tensile properties indicating comparable forming behaviour. Uniaxial, plane and biaxial strain conditions were investigated by tensile, cup drawing and stretch forming tests and the forming behaviour of all materials was simulated by FEA. From this a simple material model based on the hardening curve that neglected the differences in microstructure was used. By comparison with the experimental results the accuracy of the FEA predictions was analysed.

2. Material and Methodology

2.1 Material

The three steel types investigated in this study are HSLA, DP and TRIP. Their individual measured thicknesses and chemical compositions, as given by the supplier, are shown in Table 1.

Table 1: Measured thickness and chemical composition ranges of HSLA, DP and TRIP steels

Designation	Thickness (mm)	Chemical Composition, %				
		C	Si	Mn	P	S
HSLA	2.00	0.13 max	1.32 max	1.60 max	0.025 max	0.010 max
DP	1.97	0.15 max	1.50 max	2.00 max	0.025 max	0.010 max
TRIP	2.04	0.21 max	2.20 max	1.80 max	0.025 max	0.010 max

2.2 Methodology

The forming behaviour in uniaxial, plane and biaxial strain of the three steel types was determined by tensile, cup drawing and stretch forming tests. The thinning of all materials during forming was measured and necked as well as cracked regions of the formed samples were closely studied using optical microscopy. To investigate whether the forming and thinning behaviour of the different steels can be accurately predicted by a simple macro FEA approach, the cup and stretch forming tests were simulated using FEA and compared to the experimental results.

2.2.1 Tensile test

The tensile tests were performed as recommended in Australian standard AS 1391-1991 on specimens (Figure 1 and Table 2) oriented along the rolling direction. Since significant anisotropy was observed in the cup tests performed on the HSLA, the tensile properties of the HSLA were additionally tested in the transverse and 45^0 direction. A non-contact extensometer with a test range of 25±5mm was used. The tests were performed in a 30 kN MTS. All specimens were marked by two white dots, and situated 25 mm apart from each other on the flat gauge section. Using a camera system the displacement of the dots during testing was measured giving the force displacement curve. All experiments were performed using a strain rate of 2 mm/min. To investigate the necking and fracture behaviour, some tests were stopped at the initiation of necking while others were allowed to proceed till fracture.

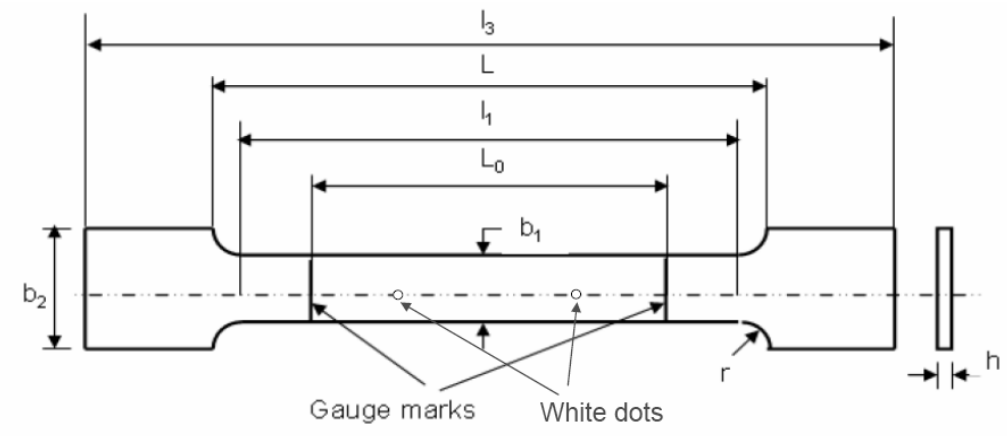

Figure 1: Standard tensile test specimen (AS 1391-1991)

Table 2: Standard tensile test specimen dimensions (AS 1391-1991)

Sections	Dimension (mm)
Gauge Length, L_0	50.0±1.0
Length of narrow parallel-sided portion, l_1	60.0
Initial distance between grips, L	63.0
Overall Length, l_3	200
Width, b_2	20.0
Width of narrow parallel-sided portion, b_1	12.5±0.6
Thickness, h	Material thickness
Radius, r	12

2.2.2 Erichsen Cup drawing

The forming behaviour, as well as the necking and fracture mode, of all materials close to plane strain was investigated in cup forming tests using an Erichsen sheet metal tester and the tool set up shown in Figure 2(a). On some specimens a circle grid was etched on the outside surface facing the die to provide strain measurements after forming. To maintain near constant friction conditions all specimens were lubricated using a combination of oil and polymer foil on the outside surface and a single layer of oil on the inside surface. For all tests a punch speed of 0.1 m/min was used. To investigate the thinning behaviour of the different steel types, cylindrical cups were drawn with a drawing ratio of 2.2 and a blankholder force of 80 kN. Additionally, cups were drawn using a drawing ratio of 2.3 and a blankholder force of 10 kN. An initial punch speed of 0.1 m/min was chosen and reduced at the end of the test to allow exact determination of the initiation of failure. For all materials these process conditions led to failure by cracking at the cup corner radius, allowing the investigation of the fracture behaviour close to plane strain.

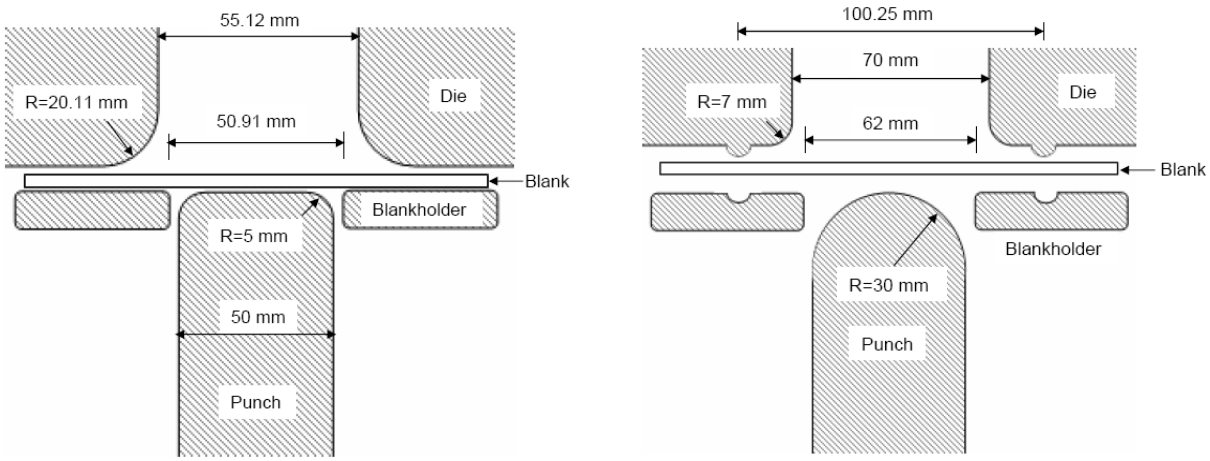

2(a) 2(b)

Figure 2: Experimental set-up of Erichsen 2(a) cup drawing and 2(b) stretch forming

2.2.3 Erichsen stretch forming

Stretch forming tests were performed using the Erichsen sheet metal tester and the tooling shown in Figure 2(b). For each test, a sandwich construction of oil together with polymer foil was used for lubrication. The punch speed and blank-holding force applied were 0.1 m/min and 230 kN, respectively. While some tests were stopped at a final punch stroke 22 mm (approximately three millimetres before the initiation of necking observed for HSLA) others were performed until fracture of the sheet. Again an initial test speed of 0.1 m/min was used and reduced to the end of the test to allow exact determination of the initiation of necking.

2.2.4 Microscopic thickness measurement

For all test conditions a small strip of the test specimen was cut perpendicular to the crack (neck). Cracks 0° and 90° to the rolling direction were observed for all materials in both the stretch and the cup forming test. Therefore the thickness distribution of the un-fractured samples was also analysed on strips cut in 0^0 and 90^0 to the rolling direction. Using a Vickers's hardness tester, marks were indented along the specimen edge in a pre-defined distance of 2 mm. This enabled the exact recording of the distances between the particular locations where the thickness measurements were taken (Figure 3b). Using an optical microscope, images of different parts of the specimen were taken. Thereby, generally at least two indentation points were present in every picture (Figure 3c). Using Image tool (version 3) software [17], the thickness of the specimen at each measurement location was determined.

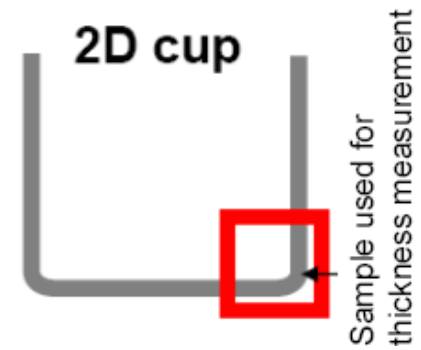

3a

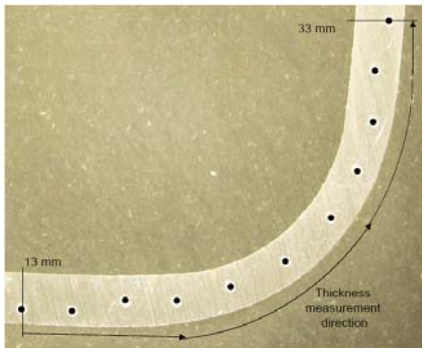

3b

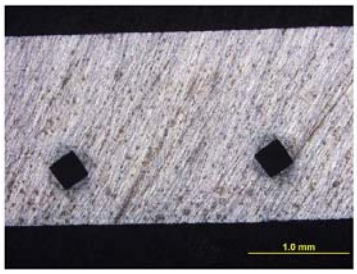

3c

3d

Figure 3: Thickness measurement method applied to the cup corner radius

2.2.5 Numerical Modelling

The cup drawing and stretch forming tests were investigated using ABAQUS/Explicit 6.5-1 with a three-dimensional model approach. The tooling was given as rigid surfaces (Figure 4), while S4R shell elements (Four node, Reduced integration) were used to mesh the blank (Figure 5). Only a quarter of the blank was used in the model because of the axis-symmetry of both tests. The average sheet thicknesses measured experimentally for the HSLA, the DP and the TRIP steel (see Table1) were detailed in the model and the true stress-strain data, determined in the tensile tests, was applied to define the material properties of the particular steel type using isotropic hardening. Since the fitted power law did not correlate well with the initial region of metal plastic definition (Figure 8), the material input used to represent the material behaviour of the three steel grades was a combination of experimental test data (initial part of the hardening curve) and material data extrapolated of the fitted power laws (later stages of the hardening curve).

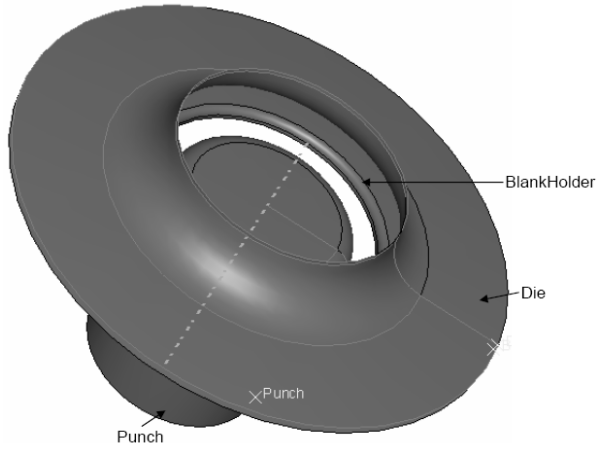

Figure 4: Rigid surfaces used in the cup forming model

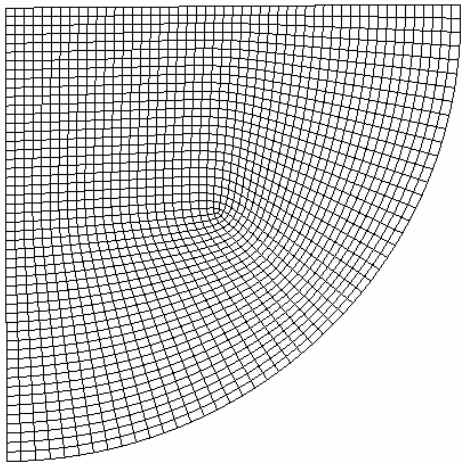

Figure 5: Axis-symmetric quarter blank used in the cup forming model

Generally, the same process parameters as present in the experimental tests were applied in the model. However, because a direct measurement of friction was not possible, a coefficient of friction giving the best possible correlation between the experimental and simulated drawing force for all materials was chosen. For the simulation of the stretch forming process the flange region of the specimen was neglected and the outside edge was fixed in the boundary conditions. This assumes a perfect clamping and no movement of the specimen between the blankholder and the die surface. Because of the high lubrication used in the stretch forming test, zero friction was assumed in the FEA approach between the blank and the punch.

To account for the anisotropic behaviour of the HSLA steel, Hills anisotropic yield criterion was used to model the material behaviour in cup drawing. In ABAQUS, anisotropic values are required in the form of stress ratios which represent the ratio between reference yield stress specified for the metal plasticity and the measured yield stress value when applied as the only non-zero stress component. R_{11}, R_{22}, R_{33}, R_{12}, R_{13} and R_{23} are anisotropic yield stress ratios in six directions of the cube element. To represent the planar anisotropy, R_{11}, R_{22} and R_{12} are important. The rest of the stress ratio values can be considered to be 1 (isotropic material behaviour). The mathematical relations used to convert the strain ratios to stress ratios (required in Abaqus to account for planar anisotropy) were (equation 1, 2 and 3).

$$R_{11} = \sqrt{\frac{r_{90}(r_0 + 1)}{r_0(r_{90} + 1)}} \qquad \text{----- (1)}$$

$$R_{22} = \sqrt{\frac{r_{90}(r_0 + 1)}{(r_0 + r_{90})}} \qquad \text{----- (2)}$$

$$R_{12} = \sqrt{\frac{3(r_0 + 1)r_{90}}{(2r_{45} + 1)(r_0 + r_{90})}} \qquad \text{----- (3)}$$

Figure 6 shows the shape of numerically drawn cup during drawing and stretching. The thickness distributions over the cup corner radius were measured for all materials as indicated by the grey line.

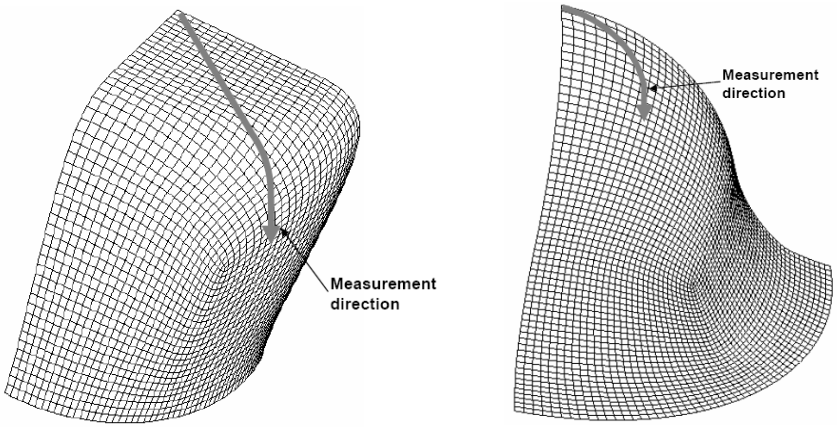

Figure 6: Simulated quarter cup during drawing and stretching

3. Results

3.1 Tensile test

The true stress-strain curves determined in the tensile test are shown in Figure 7. It can be seen that the DP steel exhibits higher initial work hardening compared to the HSLA and the TRIP steel, while the TRIP steel shows a higher UTS and maximum elongation compared to DP and HSLA. Nevertheless, compared to previous studies involving the forming behaviour of AHSS and conventional steel grades, the steels investigated in this work show very similar tensile properties. The stress strain curves of all three steel types were fitted using a power law (equation 4).

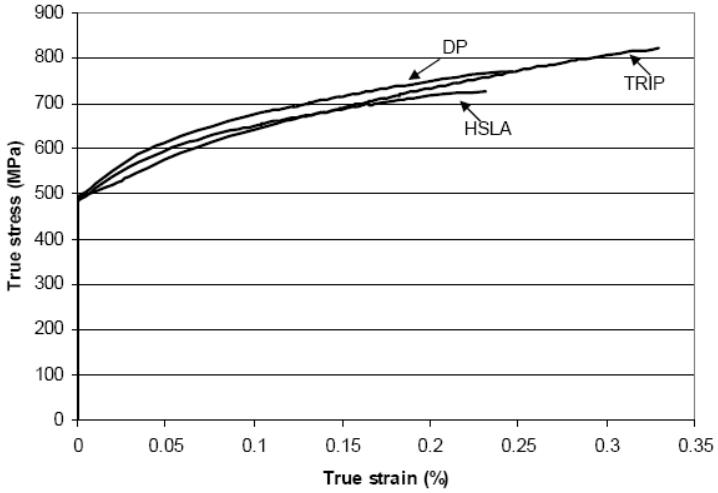

Figure 7: True stress-strain curves determined in the tensile tests for HSLA, DP and TRIP steels

$$\sigma = K\varepsilon^{n} \quad \text{----- (4)}$$

where,

σ = True stress
ε = True strain
K = Strength coefficient
n = Strain hardening exponent

The mechanical properties of all tested materials are summarized in Table. 3.

Table 3: Mechanical properties of HSLA, DP and TRIP steels

Designation	Mechanical Properties				
	Yield strength (MPa)	Tensile strength (MPa)	Elongation, %	K (MPa)	n
HSLA	483	726	28	900	0.1420
DP	491	771	30	965	0.1585
TRIP	490	821	37	1030	0.2076

Figure 8 compares the experimental true stress-strain curves with the fitted power laws. It is clear that for all materials the fitted power laws do not give a good representation of near yield behaviour. This is, because a tensile region above 10% strain was used to determine the hardening exponent.

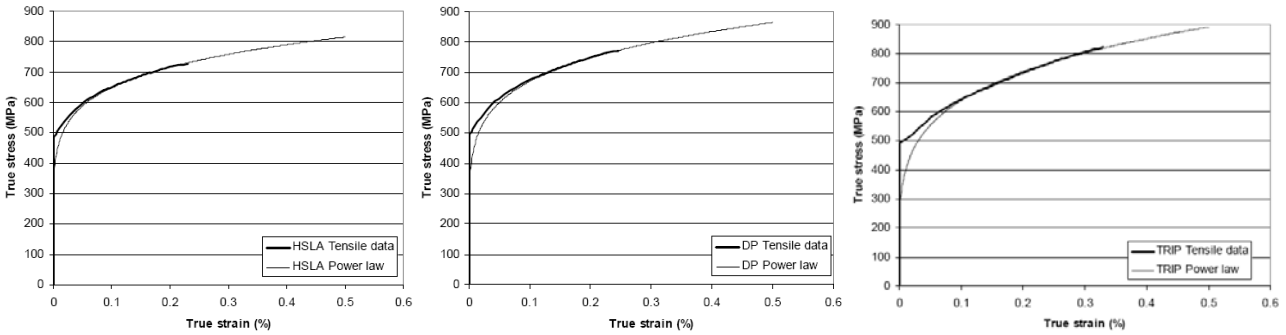

Figure 8: Experiment true stress-strain curves fitted with the power law

The anisotropic values determined for the HSLA steel are shown in Table 4. The plastic strain ratio in the rolling, 45^0 and 90^0 to rolling direction are indicated with the nomenclature of r_0, r_{45} and r_{90}, respectively. It is clear that the plastic strain ratio at 45^0 to the rolling direction is higher than the other two material directions. This indicates that thinning will be higher in the rolling and transverse direction than the 45^0 direction. The value of normal anisotropy '$\bar{r}$' determines the average depth of deepest draw possible. The planar anisotropy 'Δr' value determines the extent of earing. If Δr is less than zero, ear formation occurs near $\pm 45^0$, which was observed in cups drawn from the HSLA steel.

Table 4: Anisotropic values for HSLA steel

r_0	r_{45}	r_{90}	$\bar{r}$	Δr
0.471	1.339	0.671	0. 955	-0. 768

3.2 Cup drawing

The cups formed from the three steel types using a drawing ratio of 2.2 and a blankholder force of 80 kN are shown in Figure 9. Significant earing was observed for the HSLA while the cups drawn of DP and TRIP steel only showed minor planar anisotropy.

Figure 9: Experimental cups during drawing (Drawing ratio = 2.2)

Similar drawing forces were determined for the TRIP and DP steel, while lower forces were required to form the HSLA steel (Figure 10).

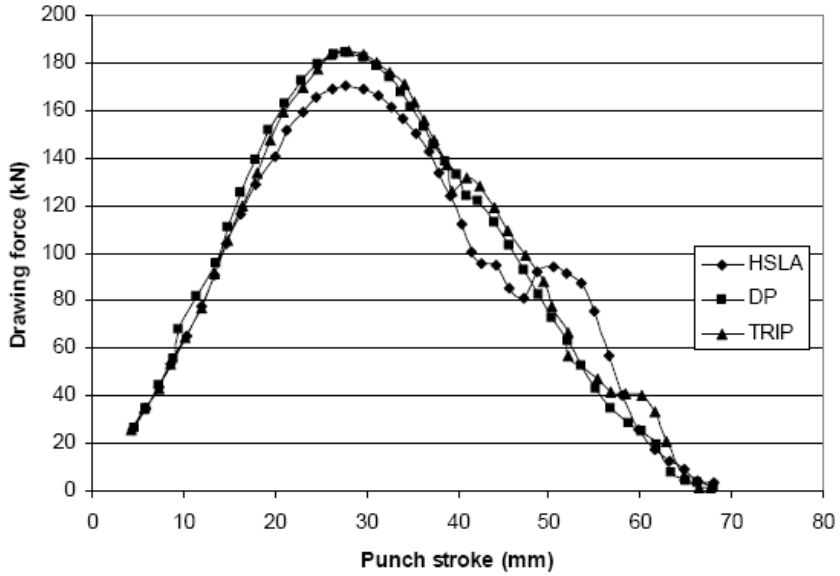

Figure 10: Experimental force displacement determined in the cup test for drawing ratio of 2.2

The thickness distribution over the cup corner radius was measured for all materials. For this a strip was cut from the punch corner radius region and prepared using the method described in section 2.2.4. To account for the differences in initial thickness between the HSLA, the DP and the TRIP steels, in Figure 11 the thickness distribution over the punch corner radius is given as the relative thickness; this is the ratio of the deformed thickness to the original material thickness. In the rolling direction the HSLA steel shows a very non uniform thickness distribution over the punch corner radius, while the thinning of the two AHSS appears to be more uniform. For 90º to the rolling direction the HSLA thins less and more uniformly, comparable to the two AHSS. In both directions the TRIP steel shows higher thinning compared to the DP steel.

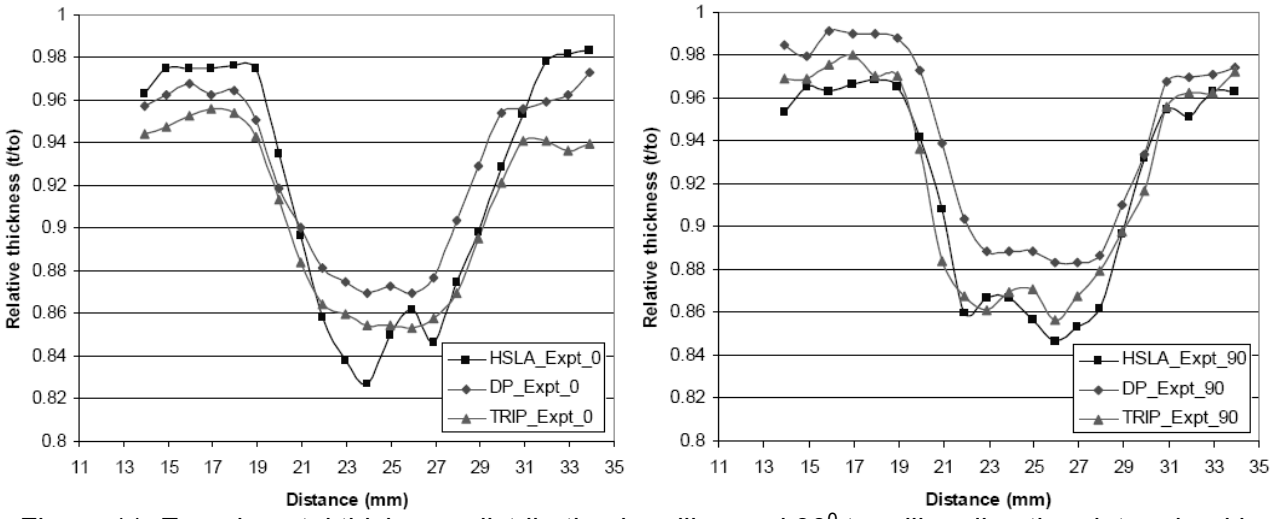

Figure 11: Experimental thickness distribution in rolling and 90^0 to rolling direction determined in the cup drawing tests using a drawing ratio of 2.2 and a blankholder force of 80kN

3.3 Stretch forming

In the stretch forming tests the TRIP steel showed the highest formability compared to DP and HSLA (Figure 12). While the HSLA could only be formed to a maximum cup height of 25 mm, the maximum cup heights achieved for DP and TRIP steel were 27.5 mm and 31 mm, respectively. In all materials, fracture was orientated 0° or 90° to the rolling direction.

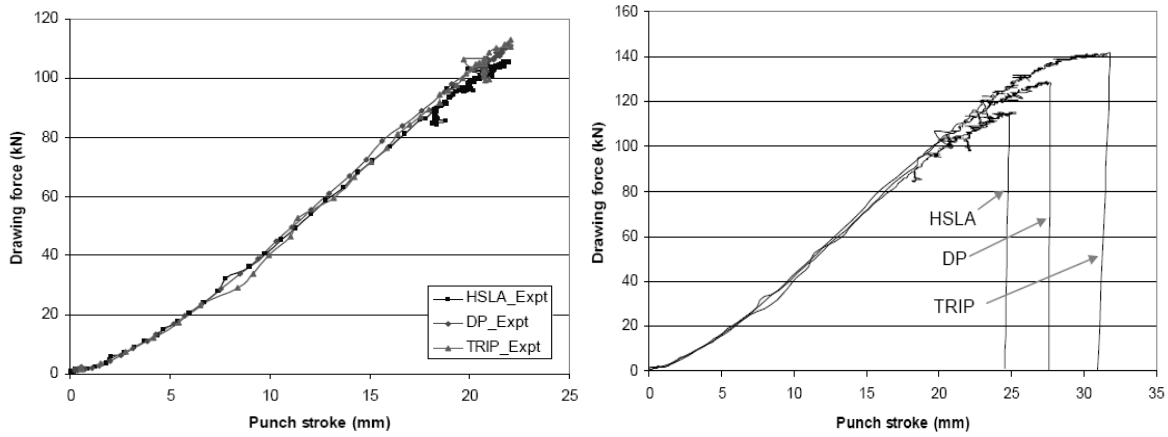

(a) (b)

Figure 12: Experimental force displacement in stretch forming for HSLA, DP and TRIP (a) at 22mm depth, (b) at fracture

To measure the thickness distribution of the un-fractured samples, a strip was cut out of the dome section 0° and 90° to the rolling direction (figure 13) and prepared as explained in section 2.2.4.

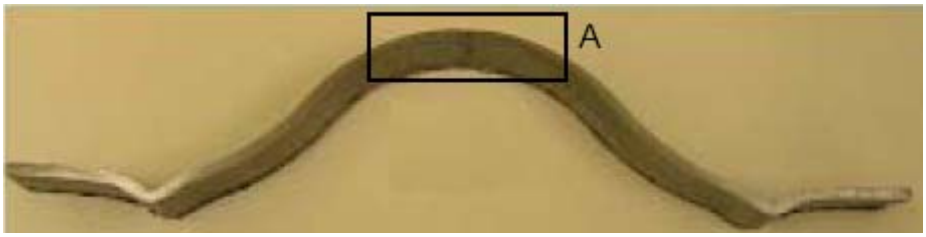

Figure 13: Cut strip in stretch forming for thickness measurement

The thickness distributions over the dome surface for region A are shown in Figure 14.

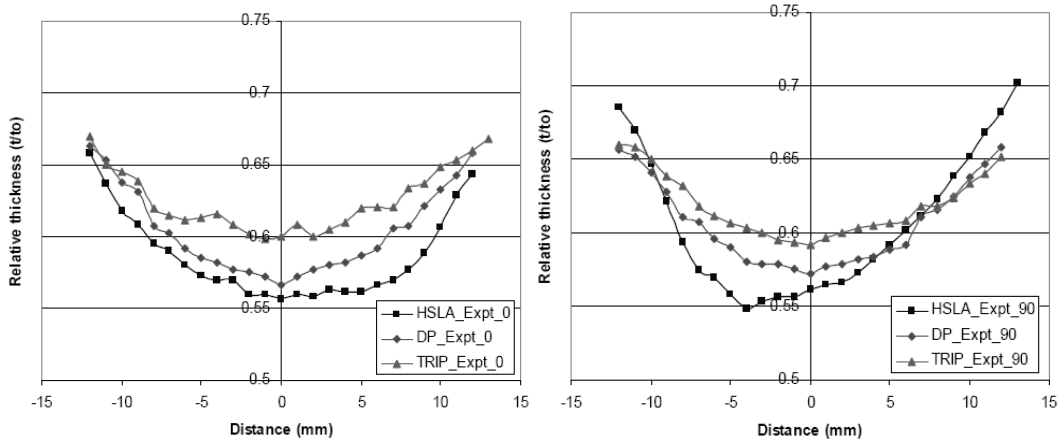

Figure 14: Experimental thickness distribution measured over the dome surface for region A for HSLA, DP and TRIP at a depth of 22mm

In contrast to the cup forming tests in stretch forming the DP steel undergoes higher thinning than the TRIP steel. In both material directions the HSLA steel shows more severe thinning than either of the AHSS. Therefore, in contrast to cup forming the thinning behaviour of the HSLA is more uniform in the rolling direction than the 90º direction.

3.4 Cup drawing simulation

In Figure 15 the force-displacement curves determined in the cup forming tests (drawing ratio of 2.2 and blankholder force of 80kN) are compared with the FEA-predictions. A good fit with the experimental results was achieved by using a friction coefficient of 0.0225 for the contact between

the die and the metal sheet (experimentally oil and foil) and 0.1 for contact at the interfaces steel sheet/BLH and steel sheet/punch (oil was used in the experiments).

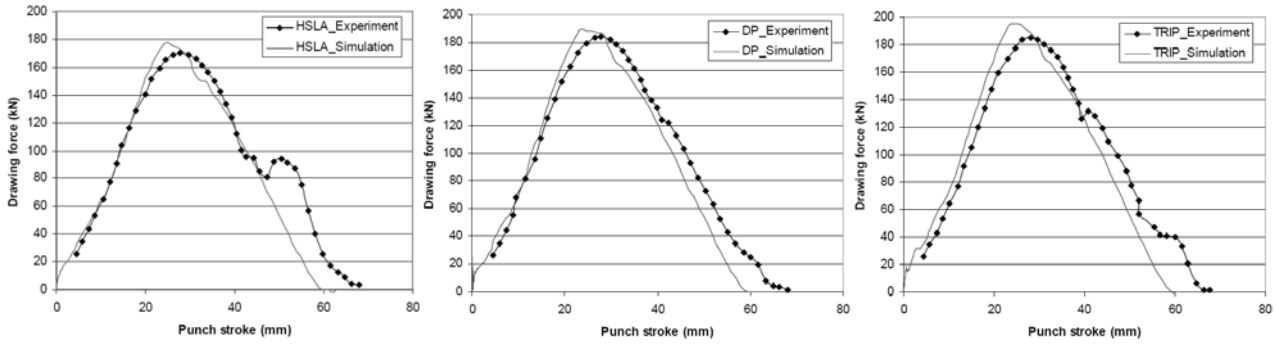

(a) (b) (c)

Figure 15: Experimental and Simulated force displacement in cup drawing test with drawing ration of 2.2 for (a) HSLA, (b) DP and (c) TRIP

The thickness distribution over the cup corner radius was numerically investigated at 0° and 90° to the rolling direction (Figure 16).

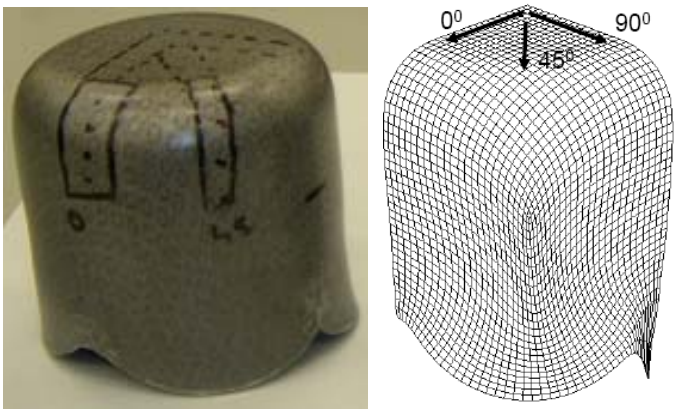

Figure 16: Experimental and Simulated thickness measurement direction in cup drawing tests with drawing ratio of 2.2 and blankholder force of 80kN

The thickness distribution over the cup corner radius predicted for strips cut of the TRIP and DP steels in the rolling direction and cut for HSLA in 0º and 90º to the rolling direction are compared to the experimental results in Figure 17.

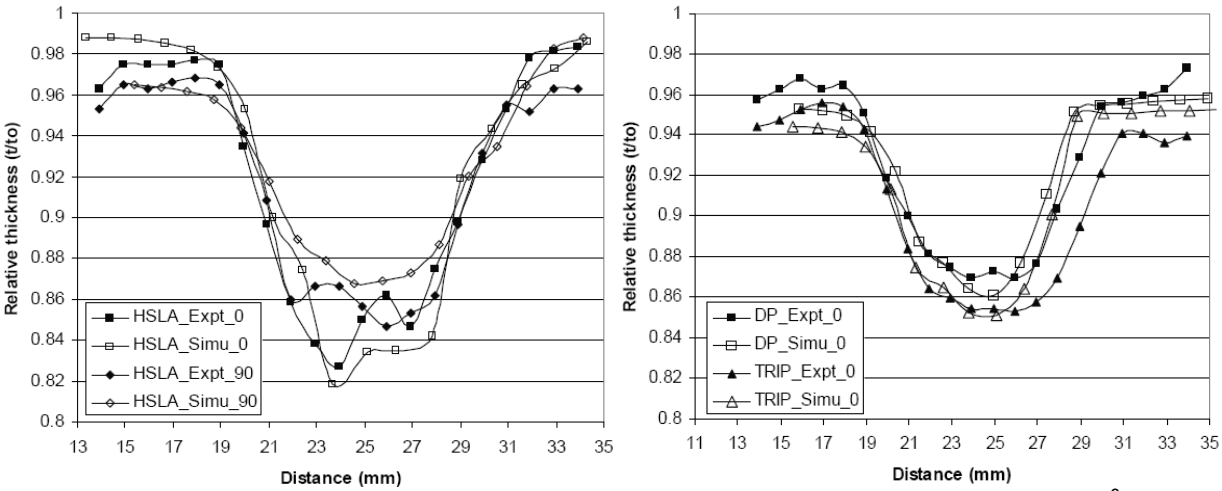

Figure 17: Experimental and Simulated thickness distribution in rolling and 90^0 to rolling direction for HSLA and rolling direction for DP and TRIP

It is clear that the FEA predictions give a very accurate representation of the thinning behaviour of all three steel types.

3.5 Stretch forming simulation

The force displacement curves numerically predicted for the stretch forming process are compared to the experimental data in Figure 18. Good correlation between the experimental results and the FEA predictions is achieved for all three steel.

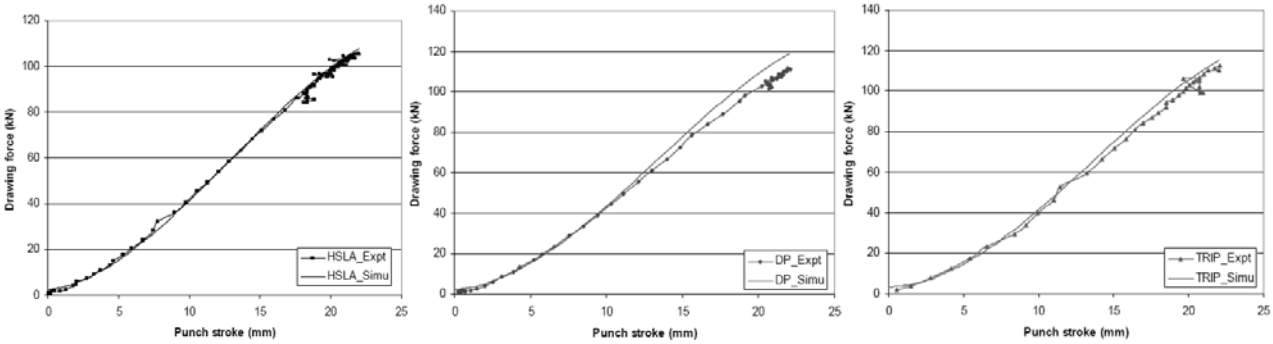

(a) (b) (c)

Figure 18: Experimental and Simulated force displacement in stretch forming (a) HSLA, (b) DP and (c) TRIP

The thickness distributions determined in the experimental tests are compared with the FEA-predictions in Figure 19.

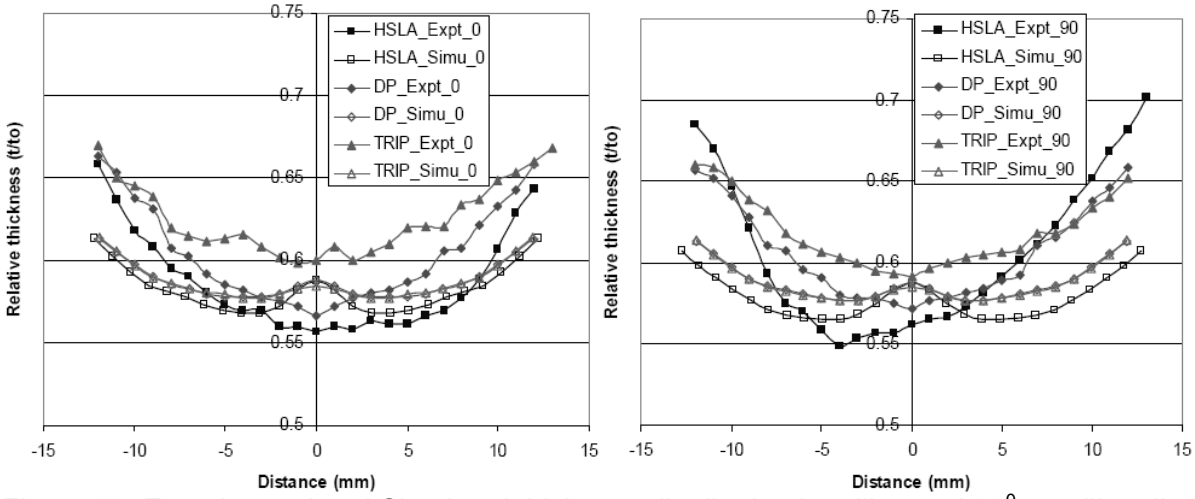

Figure 19: Experimental and Simulated thickness distribution in rolling and 90^0 to rolling direction at same individual material cup height for HSLA, DP and TRIP

There is a relatively weak prediction of thinning behaviour for all of the investigated steel types. Even so the FEA does reproduce the higher thinning of the HSLA compared to the AHSS types; although it also predicts identical relative thickness distribution for both AHSS, i.e. fails to represent the higher thinning observed for the DP compared to the Trip steel in the stretch forming test.

3.6 Fracture analysis

In section 3.4 and 3.5 it was shown that steel types with similar tensile properties can show significant differences in thinning behaviour during sheet forming. In this section the fracture behaviour of those steels is investigated for the tensile, the cup forming and the stretch forming test which approximately represents the material behaviour under uniaxial, plane and biaxial strain conditions.

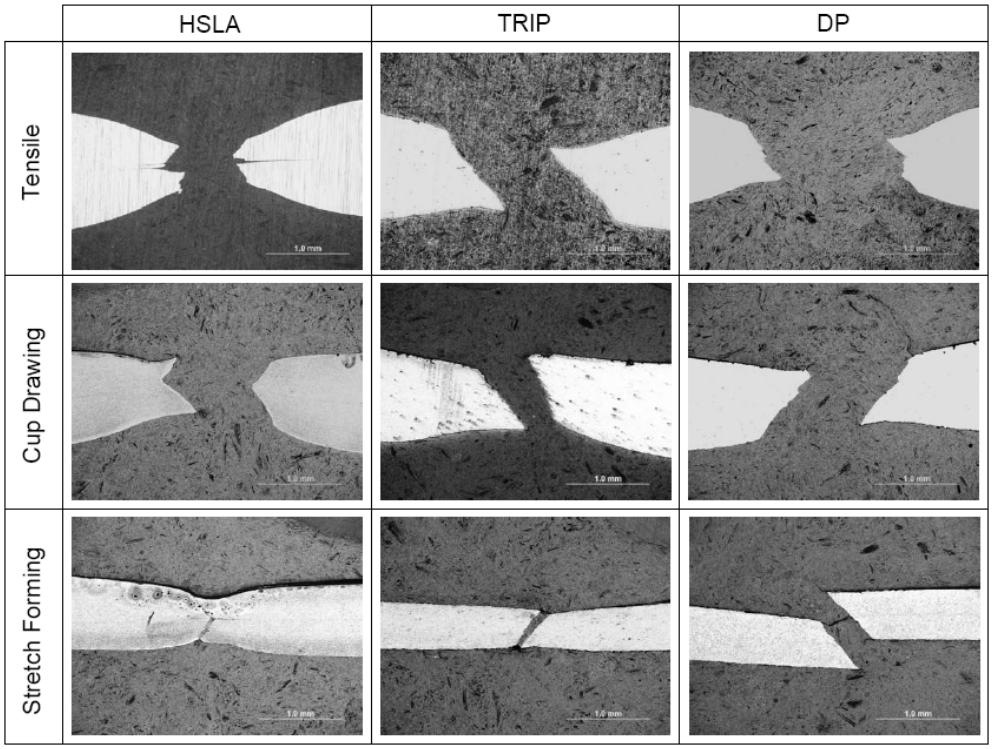

Figure 20: Fracture specimen in different strain conditions

The images for the cracked regions of all materials are shown in Figure 20. It is clear that for all materials the necking is smaller in uniaxial strain than plane strain and reduces further in biaxial strain. Out of all materials the HSLA shows the highest tendency to form a neck before fracture. While the DP steel undergoes higher necking compared to the Trip steel in uniaxial strain, no neck was observed before fracture in the stretch forming tests. In contrast to that the Trip steel showed the formation of a neck before fracture in this forming mode. In cup drawing (plane strain) the two AHSS show a similar necking behaviour.

4. Discussion

In the tensile tests it was shown that the three steel types investigated in this study have similar tensile properties suggesting a comparable forming behaviour. However, in the cup forming tests greater thinning was observed for the TRIP steel compared to the DP steel. In contrast for the stretch forming tests the opposite trend was observed, i.e. higher thinning for the DP steel compared to the TRIP steel. Additionally, the fracture analysis revealed significant differences between both steels for necking and fracture depending on the strain path. This suggests that the differences in forming might be related to differences in the microstructure. This implies that for successful simulation of the forming of these two steel types their microstructure would need to be considered in the material model. However, the FEA analysis performed using a Macro model approach (i.e. without consideration of the microstructure) gave a good representation of the forming behaviour for both steels for the cup forming test. In contrast only a weak representation of the thinning behaviour of both steels was achieved for the stretch forming tests. This indicates that while a more detailed material model that includes the microstructure might be necessary to represent the material behaviour of AHSS in stretch forming (i.e. biaxial strain) for other forming process (cup forming) a macro model is adequate.

The conventional HSLA steel showed lower formability compared to both AHSS and a significantly higher tendency to neck before fracture for all three forming conditions investigated in this study. It has to be noted that also for the HSLA using a simple macro material model a good representation of the forming behaviour in cup forming was achieved, while the FEA predictions failed to represent the forming behaviour in the stretch forming. Especially it is interesting to note the poor FEA predictions achieved for the stretch forming tests are surprising since the simple microstructure of HSLA suggest that a simple material model based hardening data sufficient to numerically represent the material properties.

Overall, this suggests that there are interesting differences between the forming modes that potentially need to be considered for all steels. To date, most work has focussed on the cup or plane strain forming (eg channels) of these steels, with relatively little attention on stretch forming.

Conclusion

The necking and fracture behaviour of a conventional HSLA steel and two AHSS for three different strain paths was determined using tensile, cup forming and stretch forming tests. While all materials showed similar tensile properties, significant differences in thinning and fracture behaviour were observed in the cup and stretch forming tests. This has been related to differences in microstructure. FEA performed for both forming processes gave a good representation of the material behaviour of all steel types for the cup drawing process. In contrast to that the FEA model failed to represent the forming behaviour of all steels for the stretch forming process. This indicates that a more sophisticated material model might be necessary to represent the forming behaviour of conventional as well as advanced high strength steels in stretch forming.

Acknowledgement

This research was supported by Deakin University. The authors gratefully extend their gratitude to Professor John L Duncan from Auckland University, New Zealand.

References

1. **Mukai, Y. (2005):** The Development of New High-strength Steel Sheets for Automobiles. KOBELCO TECHNOLOGY REVIEW NO. 26.
2. **International Iron and Steel Institute:** Project reports on UltraLight Steel Auto Body-Advanced Vehicle concepts (ULSAB-AVC), www.worldautosteel.org.
3. **Horvath, C. D. (2004):** The Future Revolution in Automotive High Strength Steel Usage. 2004, www.autosteel.org/pdfs/gdis_2004_horvath.pdf.
4. **Satorres, A. (2005):** Bending simulation of high strength steel by finite elements. Master's Thesis, University of Oulu.
5. **Bhadeshia, H. K. D. H. (2002):** TRIP-Assisted steels? ISIJ International, vol 42(9), pp. 1059-1060.
6. **Fekete, J. R. (2005):** Manufacturing Challenges in Stamping and Fabrication of Components From Advanced High Strength Steel. Int. Symp. On Niobium Microalloyed Sheet Steel for Automotive Applications, The Minerals, Metals and Material Society (TMS), pp. 1.7-115.
7. **Horvath, C. D.; Fekete, J. R. (2004):** Opportunities and Challenges for Increased Usage of Advanced High Strength Steels in Automotive Applications. Proc. Int. Symp. On Advanced High Strength Steels for Automotive Applications, Association for Iron & Steel Technology.
8. **Wagoner, R. H.; Smith, G. R. (2006):** Report Draft Advanced High Strength Steel Workshop. The Ohio State University.
9. **Fekete, J. R. (2007):** Current challenges in Implementing Advanced High Strength Steels. International Conference on Microalloyed Steels: Processing, Microstructure, Properties and Peformance, pp. 1-9.
10. **Hosford, W. F.; Caddell, R. M. (1993):** Forming Limits. Metal Forming- Mechanics and Metallurgy, Second Edition, Prentice Hall, pp. 309-325.
11. **Konieczny, A. A. (2001):** On Formability Assessment of Automotive Dual Phase Steel. International Body Engineering Conference (IBEC), SAE Technical Paper # 2001-01-3106.
12. **Sriram, S.; Yan, B.; Huang, M. (2004):** Characterization of Press Formability of Advanced High Strength Steels Using Laboratory Tests. SAE Technical Paper No. 2004-01-0506.
13. **Shi, M. F.; Gelisse, S. (year):** Issue on the AHSS forming limit Determination.
14. **International Iron and Steel Institute (2005):** ADVANCED HIGH STRENGTH STEEL (AHSS) APPLICATION GUIDELINES. Online at www.worldautosteel.org.
15. **Yamazaki, Y. (2003):** Current situation and properties of Ulta-high Strength Steel for automotive use in Japan. La Revue de Metallurgie, pp.779-786.
16. **Hasegawa, K.; Kawamura, K.; Urabe, T.; Hosoya, Y. (2004):** Effects of microstructure on stretch-flange-formability of 980MPa Grade cold-rolled Ultra High Strength Steel sheets. ISIJ International, vol. 44, no. 3, pp. 603-609.
17. http://ddsdx.uthscsa.edu/dig/itdesc.html